



King Saud University

Arabian Journal of Chemistry

www.ksu.edu.sa
www.sciencedirect.com



ORIGINAL ARTICLE

Computing and comparative analysis of topological invariants of symmetrical carbon nanotube Y junctions



Ayesha Shabbir

Preparatory Year Deanship, King Faisal University, Hofuf, Al Ahsa, Saudi Arabia

Received 25 July 2021; accepted 14 October 2021

Available online 26 October 2021

KEYWORDS

Carbon nanotubes;
Branched carbon nanotubes;
Y junctions;
Topological indices;
Bond energy;
Simple regression;
Multiple regression

Abstract Single-walled branched carbon nanotubes are highly favorable building blocks of next-generation innovative nanoelectronics and nanodevices. Y junctions as members of this family have shown great potential for the production of nanoscale three-terminal devices and carbon nanotube networks. The bond energy is among the most essential thermophysical quantities to be considered when studying chemical materials for different purposes in various fields of science and technology. To estimate the bond energy of symmetrical single-walled armchair carbon nanotube Y junctions, we are presenting a mathematical formula defined in structural parameters of Y junctions. Moreover, some linear, multiple linear and non-linear regression models described in terms of some topological indices have been presented. According to the best of our knowledge and literature, this is the first such report about this family of junctions.

© 2021 The Author. Published by Elsevier B.V. on behalf of King Saud University. This is an open access article under the CC BY license (<http://creativecommons.org/licenses/by/4.0/>).

1. Introduction and preliminaries

Branched or non-straight carbon nanotubes (CNTs) such as X, Y, T, and L are of great interest in various fields of science. Especially, in carbon nanoscience and technology where they are considered as a building block of innovative nanodevices and next-generation nanoelectronics, not just due to their excellent properties but also the need for devices produced on the nanometer scale with better mechanical properties in

comparison to straight CNTs (Liu et al., 2010; Papadopoulos et al., 2000; Kim et al., 2006; Menon and Srivastava, 1997; Aiyiti et al., 2018; Zhang et al., 2018; Mei and Cheng, 2020; Ghorbanpour-Arani et al., 2017; Yang et al., 2012; Yang et al., 2014; Meunier et al., 2002). We refer the reader to (Terrones et al., 2002; Baughman et al., 2004) for the progress and techniques made toward welding CNTs to obtain novel architectures.

The first proposed branched CNT was of Y shape; commonly known as three-terminal junction or Y junction. It was a theoretical structural model of a symmetrical armchair single-walled carbon nanotubes (SWCNTs) Y junction which appeared in Scuseria, 1992; Chernozatonskii, 1992, independently, just over a year after the discovery of the first CNT (Iijima, 1991) in 1991. Any such junction is a highly suitable candidate for the production of nanoscale electronic devices

E-mail addresses: ashinori@hotmail.com, asahmad@kfu.edu.sa
Peer review under responsibility of King Saud University.



Production and hosting by Elsevier

with better switching and reliable transport properties at room temperature. These junctions were observed experimentally (Zhou and Seraphin, 1995) in 1995. In a Y junction, three CNTs join each other in a Y-shaped pattern and generate six heptagons along with hexagons at the branching points. The position of heptagons in Y junctions determines their shape. Depending on the selection of joined CNTs, a Y junction is classified as an armchair, zig-zag, or chiral CNTs Y junction. Further, it may be single- or multi-walled, capped or uncapped, symmetric or asymmetric, metallic or semiconductor. We refer to (Zsoldos et al., 2004; Zsoldos et al., 2005; Zsoldos and Kakuk, 2007; Dimitrakakis et al., 2008; László, 2005; László, 2005; László, 2008; Materials, 2013; Yin et al., 2006) for subsequent models and variations in the constructions of Y junctions and to (Bandaru, 2012; Chernozatonskii, 2003) for some studies related to the properties and applications of Y junctions.

A molecular graph is a graphical representation of the structural formula of a chemical compound in which vertices and edges correspond to atoms and bonds, respectively. A graph invariant obtained from a molecular graph to describe quantitative structural-property relationship and quantitative structural-activity relationship of the underlined molecule is known as a *topological index (topological descriptor)*. Since it is a structural invariant hence, does not depend on the labeling or the pictorial representation of a molecular graph. Topological descriptors realized wide applications in the correlation and the prediction of numerous chemical properties (Balaban et al., 1993; Rouvray, 1988) and in experiments of comparison and isomorphism (Randić et al., 1990; Diudea, 1994).

Hyper Zagreb index (Shirdel et al., 2013), first and second multiple Zagreb indices (Ghorbani and Azimi, 2012), and augmented Zagreb index (Furtula et al., 2010) are among the long list of those Zagreb indices which are modified versions of first and second Zagreb indices (Gutman and Trinajstic, 1972). The first and second Zagreb indices are the oldest vertex-degree based topological descriptors and have shown great applications in chemical graph theory. In (Rajasekharaiyah and Murthy, 2020), it is proven that the correlation of the boiling point of benzenoid hydrocarbons are better with hyper Zagreb index than distance-based indices and, within a set of selected vertex-degree based indices augmented Zagreb index has shown best correlation with standard heat of transformations and normal boiling points of octane isomers (Gutman and Tošović, 2013). Regarding applications of multiple Zagreb indices we refer to (Réti and Gutman, 2012), whose topic of discussion is the relation of multiplicative Zagreb indices with first and second Zagreb indices. For other details of these indices, we recommend (Basavanagoud and Patil, 2016; Gutman and Trinajstic, 1972; Gutman et al., 2015; Nezhad and Azari, 2016; Wang et al., 2012; Huang et al., 2012).

The mathematical expressions of these indices are defined as follows:

Let G be a connected finite simple molecular graph with the vertex set $V(G)$ and the edge set $E(G)$. The number of atoms/vertices in G is called the *order/cardinality* of G and is denoted by $|V(G)|$. The number of bonds/edges is called the *size* of G and is represented by $|E(G)|$. The *degree of a vertex* $\mu \in V(G)$ denoted by $\partial(\mu)$ is the number of edges attached to the vertex μ and an edge $\mu\nu \in E(G)$ is called of type (s, t) if $\partial(\mu) = s$ and $\partial(\nu) = t$. For an edge $\mu\nu \in E(G)$, we define

Hyper Zagreb Index:

$$HM(G) = \sum_{\mu\nu \in E(G)} (\partial(\mu) + \partial(\nu))^2. \quad (1)$$

First multiple Zagreb Index:

$$PM_1(G) = \prod_{\mu\nu \in E(G)} (\partial(\mu) + \partial(\nu)). \quad (2)$$

Second multiple Zagreb index:

$$PM_2(G) = \prod_{\mu\nu \in E(G)} (\partial(\mu) \times \partial(\nu)). \quad (3)$$

Augmented Zagreb index:

$$AZI(G) = \sum_{\mu\nu \in E(G)} \left(\frac{\partial(\mu) \times \partial(\nu)}{\partial(\mu) + \partial(\nu) - 2} \right)^3. \quad (4)$$

2. Aim and methodology

There are recent theoretical studies on structural and electronic effects of finite size zigzag or armchair CNTs of various diameters and lengths (Pérez-Guardiola et al., 2019), their charge polarization (Fedoseeva et al., 2018), the effect of doping (Santidrián et al., 2019), and the role of tube chirality on the diffusion of water (Sam et al., 2019). There have also been studies of the properties of hybrid SWCNTs with other materials, mostly carbon materials, transition metals, and even confined water molecules (Chutia et al., 2012). However, there are relatively few computational studies of the thermodynamic of CNTs as a function of their radius, diameter, chirality, functionalization, and doping. Thus, understanding the thermodynamic properties for SWCNTs and armchairs is highly essential. Among these thermodynamic properties, bond energy or bond dissociation enthalpy for the formation of CNTs from carbon atoms has been the subject of focused research. These studies could provide a pathway to make a correlation between grown CNTs and their size which resulted in tuning their thermodynamical properties for various applications (Rodriguez et al., 2014). Furthermore, the connection of small molecule properties to infinite length can be established by mapping such properties versus length, yielding an essential basis for understanding properties in the nanosize regime.

Correlation analysis helps in assessing the strength of the relationship between two variables while regression analysis, on the other hand, provides ways to model this relationship. A regression equation in a regression model is not only used to study the relationship between variables but is also an effective tool to predict or estimate one value in terms of the others.

Here first, we describe a mathematical formula in terms of structural parameters (length and chirality of used CNTs) to compute bond energy of some symmetrical SWCNTs Y junctions. After that, few regression models as estimators for bond energy have been described. Regression models presented here are not limited to linear regression. Bilinear and non-linear regression models have also been developed. Topological indices, namely, hyper Zagreb, first and second multiple Zagreb, and augmented Zagreb indices are being used as independent variables along with structural parameters of Y junctions.

In the next section, the molecular graph of the considered type of Y junctions has been described. Section 4 is devoted

to the results. A summary of the results is given in Section 5. Lastly, references have been listed.

3. Y-junction Graphs

SWCNTs are uniquely determined by their chiral vector $v = pv_1 + qv_2$, where p and q are non-negative integers and v_2 and v_2 are the graphene sheet lattice vectors. If $p = q$, then the corresponding SWCNT is called *armchair* and denoted by (p,p) -armchair SWCNT. These tubes are always metallic.

Let l, l' , and p be positive integers such that $p \geq 4$ is an even integer and $l' = l + \frac{p}{2}$ for $l \geq 1$. If $T_{l'}$ stands for an ideal (p,p) -armchair SWCNT of length l' (layers of carbon in the tube) with uniform carbon-carbon (C-C) bond length b_{cc} . Then by $J_l(p,p)$, we mean the molecular graph of a symmetrical Y-shaped SWCNTs junction $Y_l(p,p)$ with branch length l . The junction $Y_l(p,p)$ is built by the covalent interconnection of three copies of $T_{l'}$ which intersect each other at an angle of 120° and having no ring of hexagons between pairing heptagons (Nagy et al., 2016). In $Y_l(p,p)$, we have $\frac{3}{4}p^2 - \frac{3}{2}p + 2 + 3lp$ hexagonal rings along with six heptagons. The opening of any branch in $Y_l(p,p)$ is equal to the diameter $3pb_{cc}/\pi$ of $T_{l'}$, and hydrogen-carbon (H-C) bonds are located at the edges of branches. Note that the graph $J_l(p,p)$ is describing only the (C-C) bonds.

The graph $J_l(p,p)$ is of order $\frac{3}{2}p^2 + 3p + 6 + 6lp$ and of size $\frac{9}{4}p^2 + \frac{3}{2}p + 9 + 9lp$. It has $6p$ vertices of degree two and $\frac{3}{2}p^2 - 3p + 6 + 6lp$ vertices of degree three. One such graph has depicted in Fig. 1.

4. Results and Discussion

If $p \geq 4$ is an even integer and $l \geq 1$, then the chemical formula of $Y_l(p,p)$ is C_rH_{6p} , where $r = |V(J_l(p,p))|$ is the number of carbon atoms in $Y_l(p,p)$.

To estimate bond energy of $Y_l(p,p)$, we generate a new graph $J'_l(p,p)$ (satisfying chemical structure of $Y_l(p,p)$) from $J_l(p,p)$ by attaching $6p$ vertices of degree one (representing hydrogen atoms in $Y_l(p,p)$) to degree two vertices of $J_l(p,p)$. The graph $J'_l(p,p)$ consists of $6p$ edges of type (1,3) and

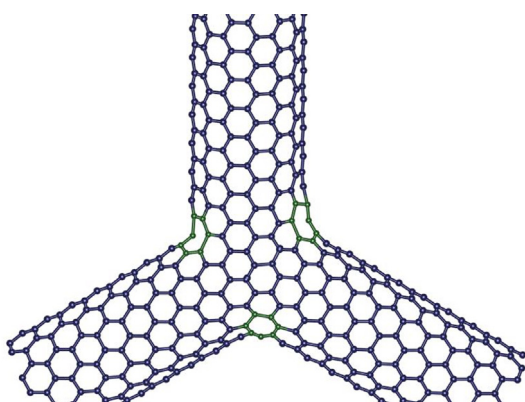


Fig. 1 A symmetrical uncapped single-walled armchair carbon nanotubes Y-junction.

$|E(J_l(p,p))|$ edges of type (3,3), which represents (H-C) and (C-C) bonds in $Y_l(p,p)$, respectively. Note that in these $|E(J_l(p,p))|$ (C-C) bonds, $\frac{3}{2}p^2 + 6 + 6lp$ are single and $\frac{3}{4}p^2 + \frac{3}{2}p + 3 + 3lp$ are double bonds.

4.1. Bond energy of $Y_l(p,p)$ in terms of p and l

The average bond length 1.42\AA of (C-C) bonds of SWCNTs is well established (Mashregi and Moshksar, 2010) and it is nearer to 1.39\AA of benzene than 1.54\AA of the diamond. Therefore, for calculations, the bond energy 518kJ/mol of (C-C) double (partial) bond of benzene is considered.

If E_Y stands for actual (experimental) bond energy of $Y_l(p,p)$. Then, for (H-C) bond energy $e_{ch} = 412\text{kJ/mol}$ and (C-C) bond energy $e_{cc} = 518\text{kJ/mol}$, the estimated bond energy E_b of $Y_l(p,p)$ is

$$\begin{aligned} E_b &= 6pe_{ch} + |E(J_l(p,p))|e_{cc} \\ &= (1165.5p^2 + 3249p + 4662 + 4662lp)\text{kJ/mol}, \end{aligned} \quad (5)$$

a quadratic equation defined for arbitrary values of p and l . Two graphs of E_b have illustrated in Fig. 2.

4.2. Regression models based on Topological indices

A regression model with one dependent and one independent variable is called simple otherwise, multiple. And, we call it non-linear if not linear. Eq. 5 is quadratic in two variables. Hence, the regression models with regression equations simpler than Eq. 5 are simple linear, bilinear and simple quadratic.

If x and y are two independent variables and z is a dependent variable then following are the regression equations of described regression models:

- Simple linear: $\hat{z} = a + bx$,
- Simple non-linear: $\hat{z} = c + dx + ex^2$,
- Bilinear: $\hat{z} = f + gx + hy$,

where a, b, c, d, e, f, g , and h are regression coefficients.

From Eq. 5, it is evident that the above-mentioned regression models with independent variables p or l , cannot be used as estimators for E_b . Therefore, another variable is needed along with these two. For this purpose, hyper Zagreb, first and second multiple Zagreb, and augmented Zagreb indices has been selected. The values of these indices for Y junction graph $J'_l(p,p)$ are as follow:

Theorem 4.1. For $p \geq 4$ an even integer and $l \geq 1$, the graph $J' = J'_l(p,p)$ has

1. $HM(J') = 81p^2 + 150p + 324 + 324lp$,
2. $PM_1(J') = 2^{\frac{9}{4}p^2 + \frac{27}{2}p + 9lp + 9} \cdot 3^{\frac{3}{2}p^2 + \frac{3}{2}p + 9lp + 9}$,
3. $PM_2(J') = 3^{\frac{9}{4}p^2 + 9p + 18 + 18lp}$,
4. $AZI(J') = \frac{6561}{256}p^2 + \frac{4779}{128}p + \frac{6561}{64} + \frac{6561}{64}lp$.

Proof 1. Since J' consists of $6p$ edges of type (1,3) and $\frac{9}{4}p^2 + \frac{3}{2}p + 9 + 9lp$ edges of type (3,3). Therefore, for these values of edges Eqs. (1)–(4) convert into

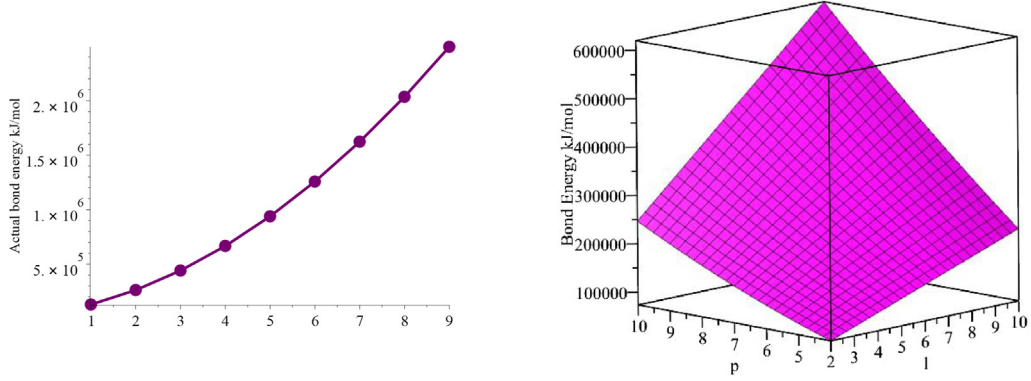


Fig. 2 Graphs of E_b .

$$\begin{aligned} HM(J') &= \sum_{\mu v \in E(J')} (\partial(\mu) + \partial(v))^2 = 16(6p) + 36\left(\frac{9}{4}p^2 + \frac{3}{2}p + 9 + 9lp\right) \\ &= 81p^2 + 150p + 324 + 324lp, \end{aligned}$$

$$\begin{aligned} PM_1(J') &= \prod_{\mu v \in E(J')} (\partial(\mu) + \partial(v)) = 4^{6p} \cdot 6^{\frac{9}{4}p^2 + \frac{3}{2}p + 9 + 9lp} \\ &= 2^{\frac{9}{4}p^2 + \frac{27}{2}p + 9lp + 9} \cdot 3^{\frac{9}{4}p^2 + \frac{3}{2}p + 9lp + 9}, \end{aligned}$$

$$\begin{aligned} PM_2(J') &= \prod_{\mu v \in E(J')} (\partial(\mu) \times \partial(v)) = 9^{\frac{9}{4}p^2 + \frac{3}{2}p + 9 + 9lp} \\ &= 3^{\frac{9}{4}p^2 + 9p + 18 + 18lp}, \end{aligned}$$

$$\begin{aligned} AZI(J') &= \sum_{\mu v \in E(J')} \left(\frac{\partial(\mu) \times \partial(v)}{\partial(\mu) + \partial(v) - 2} \right)^3 = \frac{27}{8}(6p) + \frac{729}{64}\left(\frac{9}{4}p^2 + \frac{3}{2}p + 9 + 9lp\right) \\ &= \frac{6561}{256}p^2 + \frac{4779}{128}p + \frac{6561}{64} + \frac{6561}{64}lp, \end{aligned}$$

respectively. Which completes the proof. \square

If HM , AZI , PM_1 and PM_2 are topological indices of $J'_l(p, p)$. Then for some $x \in \{HM, AZI, \ln(PM_1), \ln(PM_2)\}$, next are regression models defined in x and p to estimate E_b , where \ln stands for natural logarithm which is taken to control the value's size of these indices. The tables and figures have also been furnished for some particular values of l and p to observe $\varepsilon_x = E_b - \hat{E}_b(x)$, the error or difference between the actual value E_b , obtained by Eq. 5 and the corresponding estimated value $\hat{E}_b(x)$. Note that values provided in tables are measured in kJ/mol.

4.2.1. Simple linear regression models

For some $x \in \{HM, AZI, \ln(PM_1), \ln(PM_2)\}$ the simple linear regression equations defined for E_b are as follow:

$$\hat{E}_b(HM) = 410743.104442416 + 14.3901472862153HM,$$

$$\hat{E}_b(AZI) = 584169.589338305 + 45.4816508930545AZI,$$

$$\begin{aligned} \hat{E}_b(\ln(PM_2)) &= 18652.1791910486 + 236.07942723447 \\ &\quad \times \ln(PM_2), \end{aligned}$$

$$\begin{aligned} \hat{E}_b(\ln(PM_1)) &= 365.96400297172 + 289.130718761873 \\ &\quad \times \ln(PM_1). \end{aligned}$$

For the data given in Table 1, it is easy to observe that although, the zero error is not achieved in any case but $\varepsilon_{\ln(PM_1)}$ in the comparison

$$|\varepsilon_{\ln(PM_1)}| < |\varepsilon_{\ln(PM_2)}| < |\varepsilon_{HM}| < |\varepsilon_{AZI}|$$

is sufficiently low which makes $\hat{E}_b(\ln(PM_1))$, the best estimator for E_b among defined linear regression models. See Fig. 3 for illustration.

4.2.2. Simple quadratic regression models

For some $x \in \{HM, AZI, \ln(PM_1), \ln(PM_2)\}$, the described quadratic regression for E_b are

$$\begin{aligned} \hat{E}_b(HM) &= 10906.6666666731 + 14.3888888888889HM \\ &\quad + 2.13190679089337 \times 10^{-20}(HM)^2 \end{aligned}$$

Table 1 Differences between actual and estimated values of E_b for linear regression estimators.

$l; p$	E_b	$\hat{E}_b(HM)$	ε_{HM}	$\hat{E}_b(AZI)$	ε_{AZI}	$\hat{E}_b(\ln(PM_2))$	$\varepsilon_{\ln(PM_2)}$	$\hat{E}_b(\ln(PM_1))$	$\varepsilon_{\ln(PM_1)}$
5;4	129546	535937.3858	-406391.3858	707526.4863	-577980.48631	144701.0225	-15155.0225	130655.8253	-1109.8253
7;6	261918	666139.4385	-404221.4385	836812.3428	-574894.3428	275418.3415	-13500.3415	262906.6337	-988.6337
9;8	440910	842965.5684	-402055.5684	1012723.998	-571813.998	452820.4172	-11910.4172	441782.1854	-872.1854
11;10	666522	1066415.776	-399893.776	1235261.452	-568739.452	676907.2498	-10385.2498	667282.4804	-760.4804
13;12	938754	1336490.060	-397736.060	1504424.704	-565670.704	947678.8391	-8924.8391	939407.5187	-653.5187
15;14	1257606	1653188.421	-395582.421	1820213.755	-562607.755	1265135.185	-7529.185	1258157.300	-551.300
17;16	1623078	2016510.860	-393432.860	2182628.605	-559550.605	1629276.288	-6198.288	1623531.825	-453.825
19;18	2035170	2426457.376	-391287.376	2591669.254	-556499.254	2040102.148	-4932.148	2035531.093	-361.093
21;20	2493882	2883027.969	-389145.969	3047335.701	-553453.701	2497612.764	-3730.764	2494155.105	-273.105

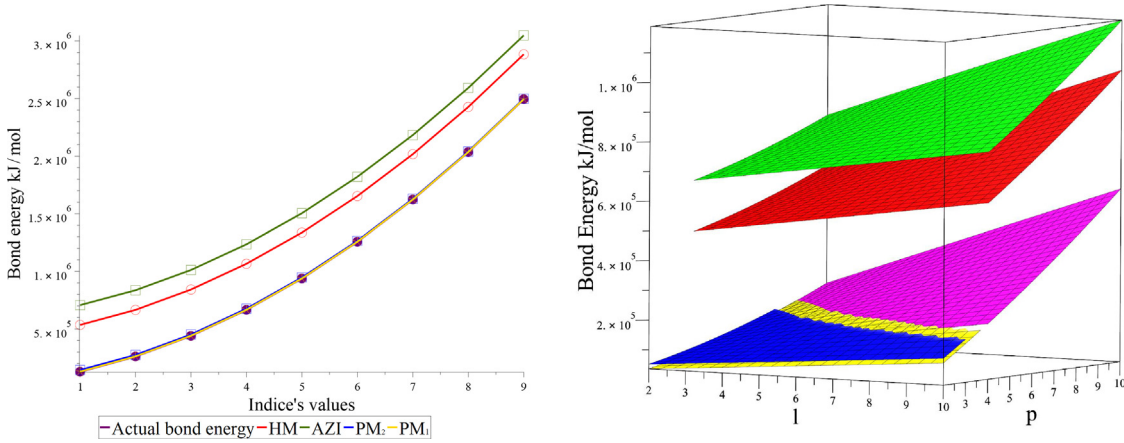


Fig. 3 Graphical comparisons of actual and estimated values of E_b for linear regression estimators.

Table 2 Differences between actual and estimated values of E_b for quadratic regression estimators.

$m; p$	E_b	$\hat{E}_b(HM)$	ε_{HM}	$\hat{E}_b(AZI)$	ε_{AZI}	$\hat{E}_b(\ln(PM_2))$	$\varepsilon_{\ln(PM_2)}$	$\hat{E}_b(\ln(PM_1))$	$\varepsilon_{\ln(PM_1)}$
5;4	129546	136090.0	-6544.0	124076.1491	5469.8509	164430.0003	-34884.00029	132642.8555	-3096.855500
7;6	261918	266280.6667	-4362.6667	254112.6599	7805.3401	294966.0003	-33048.00030	264880.2095	-2962.209500
9;8	440910	443091.3334	-2181.3334	431040.4797	9869.5203	472122.0003	-31212.00030	443737.5636	-2827.563601
11;10	666522	666522.0001	-0.0001	654854.8360	11667.1640	695898.0003	-29376.00030	669214.9177	-2692.917701
13;12	938754	936572.6668	2181.3332	925549.6915	13204.3085	966294.0002	-27540.00020	941312.2716	-2558.271603
15;14	1257606	1253243.334	4362.666	1243117.744	14488.256	1283310.0	-25704.0	1260029.625	-2423.625005
17;16	1623078	1616534.0	6544.0	1607550.426	15527.574	1646946.0	-23868.0	1625366.980	-2288.980008
19;18	2035170	2026444.667	8725.333	2018837.906	16332.094	2057202.0	-22032.00001	2037324.333	-2154.333013
21;20	2493882	2482975.334	10906.666	2476969.086	16912.914	2514078.0	-20196.00001	2495901.688	-2019.688020

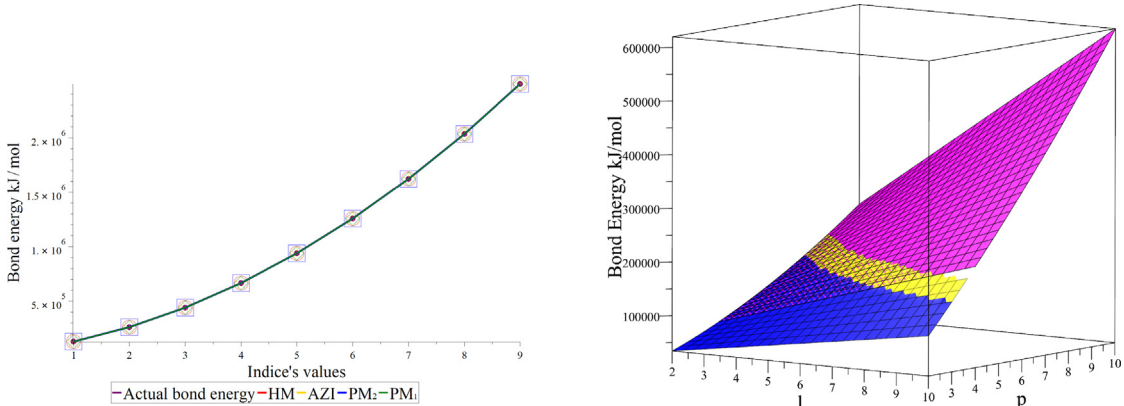


Fig. 4 Graphical comparisons of actual and estimated values of E_b for quadratic regression estimators.

$$\begin{aligned}\hat{E}_b(AZI) &= 1.60082728392449 \times 10^{-4} + 45.7473829610946 AZI \\ &\quad - 2.0060315943275 \times 10^{-7} (AZI)^2\end{aligned}$$

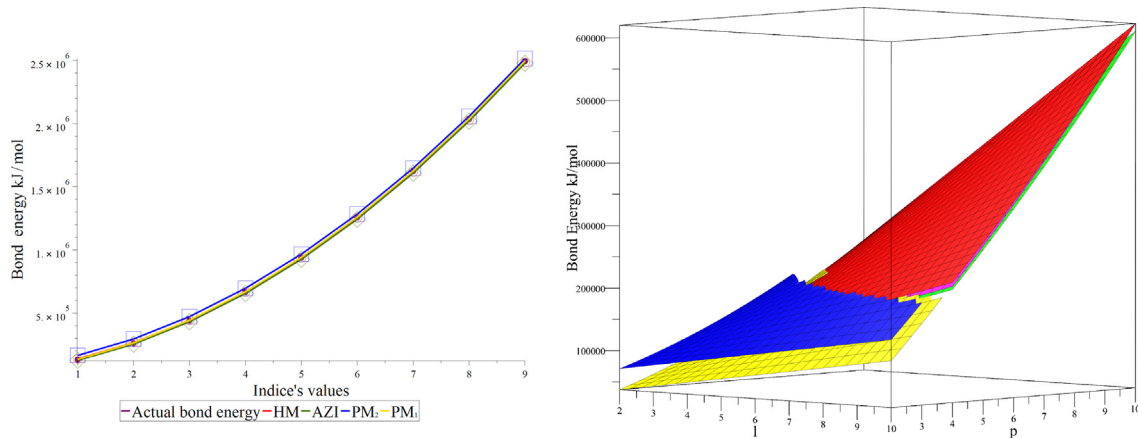
$$\begin{aligned}\hat{E}_b(\ln(PM_2)) &= 38556.0002883367 + 235.75195961445 \\ &\quad \times \ln(PM_2) - 8.67915516357 \\ &\quad \times 10^{-14} (\ln(PM_2))^2\end{aligned}$$

$$\begin{aligned}\hat{E}_b(\ln(PM_1)) &= 3366.1473086448 + 289.10130454238 \ln(PM_1) \\ &\quad - 2.65642218061376 \times 10^{-13} (\ln(PM_1))^2\end{aligned}$$

The graphs shown in Fig. 2 were the main reason for developing quadratic regression estimators with the expectation of better results. But, on comparing errors provided in Table 1 and Table 2, one can easily observe that for HM and AZI , defined quadratic equations are providing better results than corre-

Table 3 Differences between actual and estimated values of E_b for bilinear regression estimators.

$m; p$	E_b	$\hat{E}_b(HM)$	ε_{HM}	$\hat{E}_b(AZI)$	ε_{AZI}	$\hat{E}_b(\ln(PM_2))$	$\varepsilon_{\ln(PM_2)}$	$\hat{E}_b(\ln(PM_1))$	$\varepsilon_{\ln(PM_1)}$
5;4	129546	129546.0	0.0	129546.0	0.0	129545.9995	0.0005	129545.9996	0.0004
7;6	261918	261918.0	0.0	261918.0	0.0	261917.9996	0.0004	261917.9997	0.0003
9;8	440910	440910.0	0.0	440910.0	0.0	440909.9996	0.0004	440909.9995	0.0005
11;10	666522	666522.0001	-0.0001	666521.9999	0.0001	666521.9994	0.0006	666521.9995	0.0005
13;12	938754	938754.0001	-0.0001	938753.9999	0.0001	938753.9994	0.0006	938753.9997	0.0003
15;14	1257606	1257606.0	0.0	1257605.999	0.001	1257605.999	0.001	1257605.999	0.001
17;16	1623078	1623078.0	0.0	1623078.0	0.0	1623077.999	0.001	1623077.999	0.001
19;18	2035170	2035170.0	0.0	2035170.0	0.0	2035169.999	0.001	2035169.999	0.001
21;20	2493882	2493882.0	0.0	2493882.0	0.0	2493881.999	0.001	2493881.999	0.001

**Fig. 5** Graphical comparisons of actual and estimated values of E_b for bilinear regression estimators.

sponding linear equations. While, for $\ln(PM_1)$, and $\ln(PM_2)$ results are better for linear equations. The same can be observed in Fig. 4. It is also notable that linear regression equation in $\ln(PM_1)$ is still the best estimator.

4.2.3. Bilinear regression models

The bilinear regression equations defined for E_b in terms of p and $x \in \{HM, AZI, \ln(PM_1), \ln(PM_2)\}$ are as follows:

$$\hat{E}_b(HM) = 3.999975775 \times 10^{-7} + 1090.66666664p + 14.388888888889HM$$

$$\hat{E}_b(AZI) = 7.09195476814083 \times 10^{-5} + 1551.1110995875p + 45.4759945071169AZI$$

$$\begin{aligned} \hat{E}_b(\ln(PM_2)) &= -5.85988501607873 \times 10^{-4} \\ &+ 918.00004296869p + 235.75195954253 \\ &\times \ln(PM_2) \end{aligned}$$

$$\begin{aligned} \hat{E}_b(\ln(PM_1)) &= -4.57908620364488 \times 10^{-4} \\ &+ 67.322985309664p + 289.10130444179 \\ &\times \ln(PM_1) \end{aligned}$$

Table 3 and **Fig. 5**, guarantee that all four of the described bilinear regression equations are providing the best results with almost zero error in all cases. Therefore, we conclude that all these are appropriate for estimation purposes.

5. Conclusion

Formula-based simple and versatile estimators defined for arbitrary values of l and p (structural parameters of Y junctions), hyper Zagreb, first and second multiple Zagreb, and augmented Zagreb indices have been provided to determine the bond energy of symmetrical SWCNT Y junctions. Although, the best results appeared for bilinear models but it is shown that for an appropriate selection of topological indices one can achieve satisfactory results by linear models, too.

Funding

This work is supported by the Deanship of Scientific Research, King Faisal University, through the Nasher track under the grant No. 216066.

Declaration of competing interest

The authors declare that they have no known competing financial interests or personal relationships that could have appeared to influence the work reported in this paper.

References

- Aiyiti, A., Zhang, Z., Chen, B., Hu, S., Chen, J., Xu, X., Li, B., 2018. Thermal rectification in y-junction carbon nanotube bundle. *Carbon* 140, 673–679.
- Balaban, A.T., Motoc, A.T., Bonchev, I., Mekenyan, D., 1993. Topological indices for structure - activity correlations. *Top. Curr. Chem.* 114, 21–55.
- Bandaru, P.R., 2012. Carbon nanotube Y-junctions, microelectronics to nanoelectronics: Materials. Devices and Manufacturability, 277.
- Basavanagoud, B., Patil, S., 2016. A note on hyper-Zagreb index of graph operations. *Iran. J. Math. Chem.* 7, 89–92.
- Baughman, R.H., Biewer, M.C., Ferraris, J.P., Lamba, J.S., 2004. Topochemical strategies and experimental results for the rational synthesis of carbon nanotubes of one specified type. *Synth. Met.* 141 (1–2), 87–92.
- Chernozatonskii, L.A., 1992. Carbon nanotube connectors and planar jungle gyms. *Phys. Lett. A* 172 (3), 173–176.
- Chernozatonskii, L.A., 2003. Three-terminal junctions of carbon nanotubes: syntheses, structures, properties and applications. *J. Nanoparticle Res.* 5, 473–484.
- Chutia, A., Hamada, I., Tokuyama, M., 2012. Role of lone pair and π -orbital interaction in formation of water nanostructures confined in carbon nanotubes. *Chem. Phys. Lett.* 550, 118–124.
- Dimitrakakis, G.K., Tylianakis, E., Froudakis, G.E., 2008. Pillared graphene: a new 3-D network nanostructure for enhanced hydrogen storage. *Nano Lett.* 8 (10), 3166–3170.
- Diudea, M.V., 1994. Layer matrices in molecular graphs. *J. Chem. Inf. Model.* 34, 1064–1071.
- Fedoseeva, Y.V., Lapteva, L.L., Makarova, A.A., Bulusheva, L.G., Okotrub, A.V., 2018. Charge polarization in partially lithiated single-walled carbon nanotubes. *Phys. Chem. Chem. Phys.* 20, 22592–22599.
- Furtula, B., Graovac, A., Vukicevic, D., 2010. Augmented zagreb index. *J. Math. Chem.* 48, 370–380.
- Ghorbani, M., Azimi, N., 2012. Note on multiple zagreb indices. *Iran. J. Math. Chem.* 3 (2), 137–143.
- Ghorbanpour-Arani, A., Rastgoor, A., Zarei, M.S., Ghorbanpour Arani, A., Haghparast, E., 2017. Nonlocal elastic medium modeling for vibration analysis of asymmetric conveyed-fluid y-shaped single-walled carbon nanotube considering viscothermal effects. *Proc. Inst. Mech. Eng. Part C J. Mech. Eng. Sci.* 231 (3), 574–595.
- Gutman, I., Tošović, J., 2013. Testing the quality of molecular structure descriptors. Vertex degree based topological indices. *J. Serb. Chem. Soc.* 78 (6), 805–810.
- Gutman, I., Trinajstić, N., 1972. Graph theory and molecular orbitals., Total -electron energy of alternant hydrocarbons. *Chem. Phys. Lett.* 17, 535–538.
- Gutman, I., Furtula, B., Vukicevic, Z.K., Popivoda, G., 2015. On Zagreb indices and coindices. *MATCH Commun. Math. Comput. Chem.* 74, 5–16.
- Huang, Y., Liu, B., Gan, L., 2012. Augmented Zagreb index of connected graphs. *MATCH Commun. Math. Comput. Chem.* 67, 483–494.
- Iijima, S., 1991. Helical microtubules of graphitic carbon. *Nature* 354, 56–58.
- Kim, D.-H., Huang, J., Shin, H.-K., Roy, S., Choi, W., 2006. Transport phenomena and conduction mechanism of single-walled carbon nanotubes (swnts) at y-and crossed-junctions. *Nano Lett.* 6 (12), 2821–2825.
- László, I., 2005. Topological description and construction of single wall carbon nanotube junctions. *Croat. Chem. Acta* 78 (2), 217–221.
- László, I., 2005. A possible topological arrangement of carbon atoms at nanotube junctions. *Fuller. Nanotub. Carbon Nanostructures* 13 (suppl. 1), 535–541.
- László, I., 2008. Construction of carbon nanotube junctions. *Croat. Chem. Acta* 81 (2), 267–272.
- Liu, W., Meng, F., Shi, S., 2010. A theoretical investigation of the mechanical stability of single-walled carbon nanotube 3-D junctions. *Carbon* 48 (5), 1626–1635.
- Mashregi, A., Moshksar, M.M., 2010. Bond lengths and bond angles of armchair single-walled carbon nanotubes through molecular dynamics and potential energy curve approaches. *Comput. Mater. Sci.* 49, 871–875.
- Materials, Carbon, Nagy, K., Nagy, C.L., 2013. Hypergraphene from Armchair Nanotube Y Junctions, Diamond and Related Nanostructures. Series: Carbon Materials: Chemistry and Physics 6, 207–227.
- Mei, H., Cheng, Y., 2020. Research progress of electrical properties based on carbon nanotubes; interconnection. *Ferroelectrics* 564 (1), 1–18.
- Menon, M., Srivastava, D., 1997. Carbon nanotube T junctions: Nanoscale metal-semiconductor-metal contact devices. *Phys. Rev. Lett.* 79 (22), 4453.
- Meunier, V., Nardelli, M.B., Bernholc, J., Zacharia, T., Charlier, J.-C., 2002. Intrinsic electron transport properties of carbon nanotube y-junctions. *Appl. Phys. Lett.* 81 (27), 5234–5236.
- Nagy, K., Nagy, C.L., Diudea, M.V., 2016. Theoretical investigation of symmetrical three-terminal junctions. *Stud. Univ. Babes-Bolyai, Chem.* 61, 285–294.
- Nezhad, F.F., Azari, M., 2016. Bounds on hyper-Zagreb index. *J. Appl. Math. Inform.* 34, 319–330.
- Papadopoulos, C., Rakitin, A., Li, J., Vedeneev, A., Xu, J., 2000. Electronic transport in y-junction carbon nanotubes. *Phys. Rev. Lett.* 85 (16), 3476–3479.
- Pérez-Guardiola, A., Ortiz-Cano, R., Sandoval-Salinas, M.E., Fernández-Rossier, J., Casanova, D., Pérez-Jiménez, A.J., Sancho-García, J.C., 2019. From cyclic nanorings to single-walled carbon nanotubes: disclosing the evolution of their electronic structure with the help of theoretical methods. *Phys. Chem. Chem. Phys.* 21, 2547–2557.
- Rajasekharaiyah, G.V., Murthy, U.P., 2020. Hyper-Zagreb indices of graphs and its applications. *J. Algebra Comb. Discrete Appl.* 8 (1), 9–22.
- M. Randić, Design of molecules with desired properties. A Molecular Similarity Approach to Property Optimization, in Concepts and Applications of Molecular Similarity, M.A. Johnson and G.M. Maggiore, Eds. John Wiley Sons, Inc., 1990, Chap. 5, pp.77-145.
- Réti, T., Gutman, I., 2012. Relations between ordinary and multiplicative Zagreb indices. *Bull. IMVI* 2, 133–140.
- Rodriguez, K.R., Malone, M.A., Nanney, W.A., Maddux, C.J.A., Coe, J.V., Martínez, H.L., 2014. Generalizing thermodynamic properties of bulk single-walled carbon nanotubes. *AIP ADVANCES* 4 (127149), 1–15.
- Rouvray, D.H., 1988. The challenge of characterizing branching in molecular species. *Discrete Appl. Math.* 19, 317–338.
- A. Sam, V.P. K, S.P. Sathian, Water flow in carbon nanotubes: the role of tube chirality, *Phys. Chem. Chem. Phys.*, 21, 6566–6573, 2019.
- Santidrián, A., González-Domínguez, J.M., Diez-Cabanes, V., Hernández-Ferrer, J., Maser, W.K., Benito, A.M., Anson-Casaos, A., Cornil, J., Da Ros, T., Kalbáč, M., 2019. A tool box to ascertain the nature of doping and photoresponse in single-walled carbon nanotubes. *Phys. Chem. Chem. Phys.* 21, 4063–4071.
- Scuseria, G.E., 1992. Negative curvature and hyperfullerenes. *Chem. Phys. Lett.* 195, 534–536.

- Shirdel, G.H., RezaPour, H., Sayadi, A.M., 2013. The Hyperzagreb Index of Graph Operations. *Iran. J. Math. Chem.* 4 (2), 213–220.
- Terrones, M., Banhart, F., Grobert, N., Charlier, J.-C., Terrones, H., Ajayan, P.M., 2002. Molecular junctions by joining single-walled carbon nanotubes. *Phys. Rev. Lett.* 89 (7), 075505.
- Wang, D., Huang, Y., Liu, B., 2012. Bounds on Augmented Zagreb index. *MATCH Commun. Math. Comput. Chem.* 68, 209–216.
- Yang, X., Han, Z., Li, Y., Chen, D., Zhang, P., To, A.C., 2012. Heat welding of non-orthogonal x-junction of single-walled carbon nanotubes. *Phys. E Low-Dimens. Syst. Nanostructures.* 46, 30–32.
- Yang, X., Chen, D., Du, Y., To, A.C., 2014. Heat conduction in extended x-junctions of single-walled carbon nanotubes. *J. Phys. Chem. Solids* 75 (1), 123–129.
- Yin, Y., Chen, Y., Yin, J., Huang, K., 2006. Geometric conservation laws for perfect Y-branched carbon nanotubes. *Nanotechnology* 17, 4941–4945.
- Zhang, C., Akbarzadeh, A., Kang, W., Wang, J., Mirabolghasemi, A., 2018. Nano-architected metamaterials: carbon nanotube-based nanotusses. *Carbon* 131, 38–46.
- Zhou, D., Seraphin, S., 1995. Complex branching phenomena in the growth of carbon nanotubes. *Chem. Phys. Lett.* 238, 286–289.
- Zsoldos, I., Kakuk, G., 2007. New formation of carbon nanotube junctions. *Model. Simul. Mater. Sci. Eng.* 15 (7), 739–745.
- Zsoldos, I., Kakuk, G., Réti, T., Szasz, A., 2004. Geometric construction of carbon nanotube junctions. *Model. Simul. Mater. Sci. Eng.* 12 (6), 1251–1266.
- Zsoldos, I., Kakuk, G., Janik, J., Pék, L., 2005. Set of carbon nanotube junctions. *Diam. Relat. Mater.* 14 (3–7), 763–765.